Bioresources and Bioprocessing

RESEARCH

Open Access

Enhancing the thermostability and activity of uronate dehydrogenase from *Agrobacterium tumefaciens* LBA4404 by semi-rational engineering

Hui-Hui Su[1†], Fei Peng[1†], Pei Xu[1], Xiao-Ling Wu[1], Min-Hua Zong[1], Ji-Guo Yang[2] and Wen-Yong Lou[1*]

Abstract

Background: Glucaric acid, one of the aldaric acids, has been declared a "top value-added chemical from biomass", and is especially important in the food and pharmaceutical industries. Biocatalytic production of glucaric acid from glucuronic acid is more environmentally friendly, efficient and economical than chemical synthesis. Uronate dehydrogenases (UDHs) are the key enzymes for the preparation of glucaric acid in this way, but the poor thermostability and low activity of UDH limit its industrial application. Therefore, improving the thermostability and activity of UDH, for example by semi-rational design, is a major research goal.

Results: In the present work, three UDHs were obtained from different *Agrobacterium tumefaciens* strains. The three UDHs have an approximate molecular weight of 32 kDa and all contain typically conserved UDH motifs. All three UDHs showed optimal activity within a pH range of 6.0–8.5 and at a temperature of 30 °C, but the UDH from *A. tumefaciens* (At) LBA4404 had a better catalytic efficiency than the other two UDHs (800 vs 600 and 530 s^{-1} mM^{-1}). To further boost the catalytic performance of the UDH from AtLBA4404, site-directed mutagenesis based on semi-rational design was carried out. An A39P/H99Y/H234K triple mutant showed a 400-fold improvement in half-life at 59 °C, a 5 °C improvement in T_{50}^{10} value and a 2.5-fold improvement in specific activity at 30 °C compared to wild-type UDH.

Conclusions: In this study, we successfully obtained a triple mutant (A39P/H99Y/H234K) with simultaneously enhanced activity and thermostability, which provides a novel alternative for the industrial production of glucaric acid from glucuronic acid.

Keywords: Uronate dehydrogenase, Semi-rational engineering, Biocatalysis, Glucuronic acid, Glucaric acid

Background

Uronate dehydrogenase (EC 1.1.1.203, UDH), an NAD^+-like oxidoreductase, can convert uronic acids [e.g., glucuronic acid (GlcA)] into aldaric acids [e.g., glucaric acid (GA)] (Fig. 1). UDH was first found in *Agrobacterium tumefaciens* strain C58 and *Pseudomonas syringae* pv. tomato strain DC3000 (Zajic et al. 1959; Wagner and Hollmann 1976). Subsequently, UDHs were also cloned and characterized from other organisms, including *Pseudomonas putida* KT2440, *Fulvimarina pelagi* HTCC2506, *Oceanicola granulosus* DSM15982, *Streptomyces viridochromeogenes* DSM40736, *Polaromonas naphthalenivorans*CJ2 and *Thermo bispora* DSM43833 (Moon et al. 2009; Pick et al. 2015; Wagschal et al. 2015; Li et al. 2018).

Recently, UDH has attracted considerable attention as the key enzyme for GA and galactarate production from uronic acids. GA was identified as a "top value-added chemical from biomass" by the US Department of Energy in 2004 (Werpy et al. 2004) and shows considerable

*Correspondence: wylou@scut.edu.cn
†Hui-Hui Su and Fei Peng contributed equally to this work
[1] Laboratory of Applied Biocatalysis, School of Food Science and Engineering, South China University of Technology, Guangzhou 510640, People's Republic of China
Full list of author information is available at the end of the article

potential in the food and pharmaceutical industries, with applications as a food additive, dietary supplement, therapeutic medicine, agent builder and polyamide derivative (Dwivedi et al. 1990; Bespalov and Aleksandrov 2012; Walaszek 1990; Zółtaszek et al. 2008; Morton and Kiely 2000). Of all the characterized UDHs, the enzyme from *A. tumefaciens* strain C58 shows the highest catalytic efficiency (829 s^{-1} mM^{-1}) with GlcA as substrate. However, its T_{50}^{50} value is only 37 °C (Pick et al. 2015). Subsequently, Roth et al. achieved a more thermostable triple variant with a T_{50}^{15} value of 62 °C and a $\Delta\Delta G_U$ of 2.3 kJ/mol compared to wild-type (Roth et al. 2017). However, this variant still does not meet the requirements of industry.

In line with the hypothesis that conformational changes in the catalytic center during heat treatment affect enzyme activity, researchers have attempted to improve the thermostability of various enzymes by increasing the stability of the catalytic center using a structure-guided enzyme engineering approach (Tanner et al. 1996; Blair et al. 2007; Etzl et al. 2018; Zhang et al. 2016). Thus, the thermostability of α-keto acid decarboxylase, measured as the temperature at which 50% activity remains after a 1-h incubation, T_{50}^{1h}, improved by 3.3 °C compared to wild-type after structure-guided engineering of the catalytic center (Sutiono et al. 2018). Surface engineering can also increase enzyme thermostability by altering hydrogen bonds, salt bridges and hydrophobic interactions (Alponti et al. 2016; Eijsink et al. 2004; Yang et al. 2007). For example, the half-life and T_m of alkaline α-amylase from *Alkalimonas amylolytica* were raised by 6.4-fold and 5.4 °C, respectively, after introducing multiple arginines on the protein surface (Deng et al. 2014).

In this work, the enzyme characteristics of three UDHs from three *A. tumefaciens* strains were investigated. We attempted to enhance the thermostability and activity of one particular example (AtLBA4404 UDH) by generating small and smart enzyme libraries through semi-rational engineering. Analysis of the structure of the most promising variants showed that the mutated positions were mainly located in the flexible loop near the catalytic center.

Materials and methods

Bacterial strains and plasmids

Three *A. tumefaciens* strains, *A. tumefaciens* LBA4404 (AtLBA4404), *A. tumefaciens* GV3101 (AtGV3101) and *A. tumefaciens* EHA105 (AtEHA105), were used as genomic templates. The above strains were donated by Prof. Li from Guangdong Academy of Agricultural Sciences (Guangdong, China). The engineered *Escherichia coli* strains containing the target genes were cultured in Luria–Bertani (LB) broth with antibiotics (50 μg/ml kanamycin) at 37 °C. *E. coli* DH5α (Trans Gen Biotech, China) and *E. coli* BL21 (DE3) (Trans Gen Biotech, China) were used as the cloning host and expression host, respectively. The plasmid pET-28a(+) (Jierui, China) was employed as the template for overexpression of the UDHs.

Expression and purification of recombinant proteins

The preparation of genomic DNA and general cloning steps were performed as previously described (Zhu et al. 2014). We confirmed that the candidate genes of the three *A. tumefaciens* strains contained conserved UDH domain sequences by PCR and sequencing. The primers used to amplify the conserved domain sequences from their genomic DNA are shown in Additional file 1: Table S1. The three target UDH genes were digested with restriction enzymes *Hin*dIII and *Xho*I and then ligated into the corresponding restriction sites of pET-28a(+). The resulting constructs (pLBA-UDH, pGV-UDH and pEHA-UDH) were transformed into *E. coli* DH5α and positive cells were confirmed by gene sequencing.

Escherichia coli BL21 (DE3) carrying recombinant plasmids was first incubated overnight in LB medium containing kanamycin (50 μg/ml) and shaken at 37 °C and 200 rpm. Then, 1% (v/v) of these cultures were used to seed fresh LB broth medium with kanamycin (50 μg/ml) and cultured at 37 °C and 200 rpm. When the OD_{600} reached 0.6–0.8, isopropyl β-D-1-thiogalactopyranoside (IPTG, final concentration 0.2 mM) was added to trigger the expression of the target genes. After expression at 20 °C for 20–24 h, the cells were harvested at 8000×*g* for

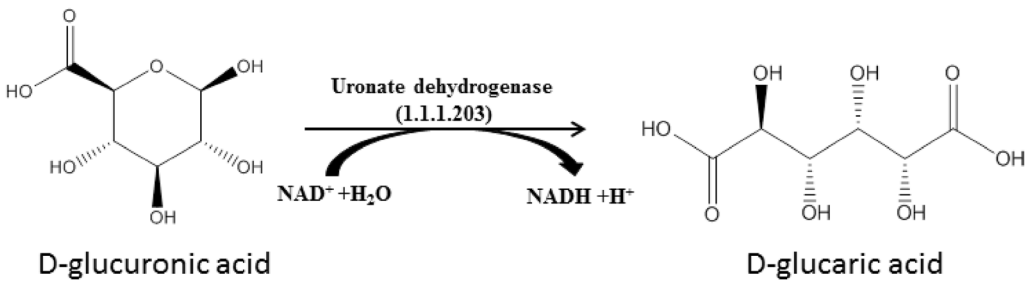

Fig. 1 Uronate dehydrogenase catalyzes a dehydrogenation reaction at C1, 6 position of glucuronic acid

10 min and resuspended in lysis buffer (20 mM Na_2HPO_4 (pH 7.4), 500 mM NaCl and 20 mM imidazole). Next, cells were sonicated and the cell homogenates were centrifuged. The supernatants were filtered and loaded onto a nickel column (Ni–NTA, Bio-Rad laboratories, Hercules, CA) using the manufacturer's instructions for purification.

Enzyme activity assay

UDH activity was measured by determining NADH generation at 340 nm and 30 °C in a potassium phosphate buffer (KPi) reaction system (50 mM, pH 8.0) containing GlcA (5 mM), galacturonic acid (5 mM) and NAD^+(2 mM). One unit of UDH activity was defined as the amount of UDH which generated 1 μmol NADH in 1 min. Protein concentration was measured using the Bradford method (Kruger 1988).

The thermostability of UDH and variants was evaluated by the parameters half-life ($t_{1/2}$) and T_{50}^{10}: $t_{1/2}$ was determined by measuring the residual activity of the enzymes at 59 °C and pH 8.0. T_{50}^{10} was defined as the temperature (50–65 °C) at which 50% of the enzyme (0.05 mg/ml) was inactivated in 10 min.

Characterization of the UDHs

The optimal pH values of the three UDHs were evaluated in the following buffer systems: citric acid–sodium citrate (pH 4.0–7.0, 50 mM), KPi (pH 7.0–9.0, 50 mM) and glycine–NaOH (pH 9.0–11.0, 50 mM). The optimal temperatures of the UDHs were also assayed in KPi buffer (50 mM, pH 8.0) with a temperature range of 4 °C–50 °C for wild-type UDH. UDH thermostability was assessed after incubation at temperatures in the range 4–50 °C for 3 h.

The effect of various metal ions, including $FeCl_2$, $FeCl_3$, $MgCl_2$, $CoCl_2$, $ZnCl_2$ and $CuCl_2$ (2 mM), on UDH activity was investigated. The effect of chemical regents Triton X-100, ethylene diamine tetra-acetic acid (EDTA), sodium dodecyl sulfate and urea on UDH activity was also tested.

The enzyme activity in the additive-free buffer was used as 100% for comparison purposes.

The kinetic parameters of the UDHs were measured using glucuronate or galacturonate as substrate at 0–10 mM in KPi buffer containing 1.2 mM NAD^+ (50 mM, pH 8.0). Similarly, kinetic analysis was performed using NAD^+ in the concentration range 0–1.5 mM in KPi buffer containing 10 mM glucuronate (50 mM, pH 8.0). The initial rate of the same enzyme concentration was evaluated for a series of different substrates. Nonlinear curve fitting was performed according to the Michaelis–Menten equation using Origin 8.0.

Site-directed mutagenesis of *A. tumefaciens* LBA4404

The UDH from AtLBA4404 was selected for further molecular modification because it showed the highest k_{cat}/K_m (800 s^{-1} mM^{-1}) of the three UDHs. A model of the UDH from AtLBA4404 was constructed by homology modeling using Swiss-model (http://swissmodel.expasy.org/) (Biasini et al. 2014) with the crystal structure of UDH from AtC58 (PDB code 3RFT) as the template (Parkkinen et al. 2011). Deep View (http://spdbv.wital-it.ch/) was used to evaluate which of the mutated amino acid positions were located on the protein surface and a default value of 30% solvent exposure was chosen.

To generate a mutant library, we performed the polymerase chain reaction (PCR) using pET28a-AtLBA4404UDH as the template and the degenerate codon NNK (Additional file 1: Table S1). *E. coli* BL21 (DE3) containing the mutant clones was grown on LB agar plates with 50 μg/ml kanamycin for 16 h. As single colony was picked and cultured in 96-deep-well plates containing medium with 100 μg/ml kanamycin and 0.05 M IPTG for 20 h at 30 °C. A culture volume of 100 μl was centrifuged (5000 rpm for 10 min at 4 °C), and the pellets were stored at − 80 °C for 4 h. Next, 50 μl lysis buffer (50 mM KPi pH 8.0) was added at 37 °C for 1 h, and then centrifuged (1000 rpm for 5 min at 4 °C). Subsequently, 50 μl supernatant was incubated in a PCR thermocycler at 30–65 °C for 10 min, then mixed with the substrate reaction solution (50 mM KPi pH 8.0, 1 mM $MgCl_2$ and 10 mM GlcA), and finally the residual activity was determined according to "Enzyme activity assay" section.

Product analysis by NMR

The synthesis of GA from GlcA by UDH was carried out in a 25 ml reaction system with 5 mg UDH, KPi buffer (50 mM, pH 8.0), 2 mM NAD^+ and 10 mM GlcA. The reaction was incubated for 30–60 min at 30 °C and then stopped with acetonitrile (1:10). The product was dissolved in D_2O for NMR analysis. 1H-NMR spectra were recorded on a Bruker 600 MHz instrument (Bruker Corporation, Fallanden, Switzerland). The spectra were obtained at 30 °C, a delay time of 10 s, and a delay time of 10 s, and an acquisition time of 2 s.

Bioconversion of GlcA with purified UDH enzyme

The reaction system was carried out in 100 ml consisting of 50 mM KPi (pH 8.0), 5 mg/l purified UDH, 10 mM NAD^+, 30 mM GlcA at 30 °C for wild-type and H99Y/H234K, or at 37 °C for A39P/H99Y/H234K, and stopped by cooling on ice. GA production was stoichiometric with NADH formation, which was monitored in a spectrophotometer by absorbance at 340 nm and 30 °C. The yields of GA were determined using a high-performance liquid chromatograph equipped with Waters 1525 refractive

index detectors (Waters, USA), and an Aminex HPX-87H column (300 mm × 7.8 mm, Bio-Rad Laboratories, Hercules, CA). The mobile phase was 5 mM H_2SO_4, and the column was eluted at 65 °C at a flow rate of 0.5 ml/min. The samples were withdrawn at different reaction points to determine the yield of product. All experiments were performed in triplicate.

Statistical analysis

Data were obtained at least in triple and expressed as mean ± standard deviation (SD). To test for statistically significant differences between conditions, an unpaired two-tailed Student's t test was applied assuming equal variance. The level of significance is indicated in figures by the following: $p < 0.01$, $p < 0.001$.

Results

Characterization of three UDH genes and their cognate enzymes

Cloning of the UDH genes from *A. tumefaciens* strains allowed us to analyze the predicted amino acid sequences of their respective enzymes. All three proteins contained characteristically conserved UDH motifs, such as GxxGxxG and YxxxK (Thomas et al. 2002; Hoffmann et al. 2007; Yoon et al. 2009). In addition, the three UDHs were very similar to that of *A. tumefaciens* C58, with a sequence identity of 89%, 98% and 98% for *A. tumefaciens* LBA4404, *A. tumefaciens* GV3101 and *A. tumefaciens* EHA105, respectively (Additional file 1: Fig. S1). Details of the three genes have been deposited at NCBI, with accession numbers MF663795 (*A. tumefaciens* LBA4404), MF663796 (*A. tumefaciens* GV3101) and MF663797 (*A. tumefaciens* EHA105).

We next prepared recombinant versions of each UDH. SDS-PAGE suggested that the molecular mass of all three enzymes was 32 kDa (Additional file 1: Fig. S2), consistent with their theoretical value as well as a previous report (Yoon et al. 2009). Purification and yield details are provided in Additional file 1: Table S2. The purified wild-type UDHs displayed the highest catalytic activity at 30 °C, but demonstrated thermal instability above 30 °C (Additional file 1: Fig. S3a, b). This limitation hinders biocatalytic applications of wide-type UDHs in industry. All three UDHs performed with relatively high enzyme activity in the pH range 6.0–8.5, with optimal activity at pH 8.0 (Additional file 1: Fig. S3c). We also measured the effect of metal ions on enzyme activity (Additional file 1: Table S3) and determined their kinetic parameters (Additional file 1: Table S4). No significant differences in the activity and thermostability of the UDHs from the three *A. tumefaciens* strains were observed. However, the UDH from *A. tumefaciens* LBA4404 showed higher kinetic efficiency (k_{cat}/K_m: 800 s^{-1} mM^{-1}) for glucuronate than the enzymes from *A. tumefaciens* GV3101 (k_{cat}/K_m: 600 s^{-1} mM^{-1}) or *A.tumefaciens* EHA105 (k_{cat}/K_m: 530 s^{-1} mM^{-1}). Therefore, the UDH derived from *A. tumefaciens* LBA 4404 was selected for further study.

Identification of target residues for mutagenesis and construction of mutant

To attempt to improve the thermostability of the UDH from *A. tumefaciens* LBA4404, we adopted a structure-guided enzyme engineering strategy, which involves mutation of key sites in the protein sequence. Initially, therefore, we constructed a homology model of UDH using Swiss-model (https://swissmodel.expasy.org/) with the UDH from *A. tumefaciens* C58 (PDB code 3RFT) as the template) (Parkkinen et al. 2011). This homology model showed that 93.12% of the residues have an averaged 3D-1D score ≥ 0.2 (Indeed, at least 80% of the amino acids scored ≥ 0.2 in the 3D-1D profile (Additional file 1: Fig. S4).

Identification of amino acid positions for mutation in At58 UDH was based on the structure-guided enzyme engineering and a previously report (Roth et al. 2017) to select target residues in the UDH from AtLBA4404. Five residues (L36, A39, E79, H99 and H234) in the UDH amino acid sequence were identified as candidates and were altered by site-directed saturation mutagenesis (Fig. 2). We found that some mutations in sites A39, H99 and H234 had a positive effect on thermostability and enzyme activity (Table 1).

To check the thermostability of the UDH mutants, enzyme solutions from engineered *E. coli* strains' cell-free supernatants were incubated in 96-well PCR plates at 58 °C for 10 min. Subsequently, the residual activity of the UDH mutants was determined. The variants of the two libraries based on L36 and E79 showed large decreases in thermostability compared to WT. In contrast, the thermostability of the A39P and H99Y variants from the A39 and H99 libraries were slightly more thermostable that wild-type UDH, which the double mutant, A39P/H99Y, performed better. H234K showed the best thermostability and specific activity compared to other variants in the H234K library and also slightly outperformed single mutants from the other libraries. When these mutants were combined, the resulting double or triple mutants showed synergistic effects, improving thermostability still further; the triple mutant A39P/H99Y/H234K performed best (Fig. 3). To define the optimal temperature and pH for the most promising variants, the double mutants H99Y/H234K and the triple A39P/H99Y/H234K were assayed across a temperature range of 30–65 °C and a pH range of 5.0–9.0 (Fig. 4). These experiments showed the optimal temperature of the mutants to be 35 °C (Fig. 4a) and the optimal pH to be 8.0 (Fig. 4b).

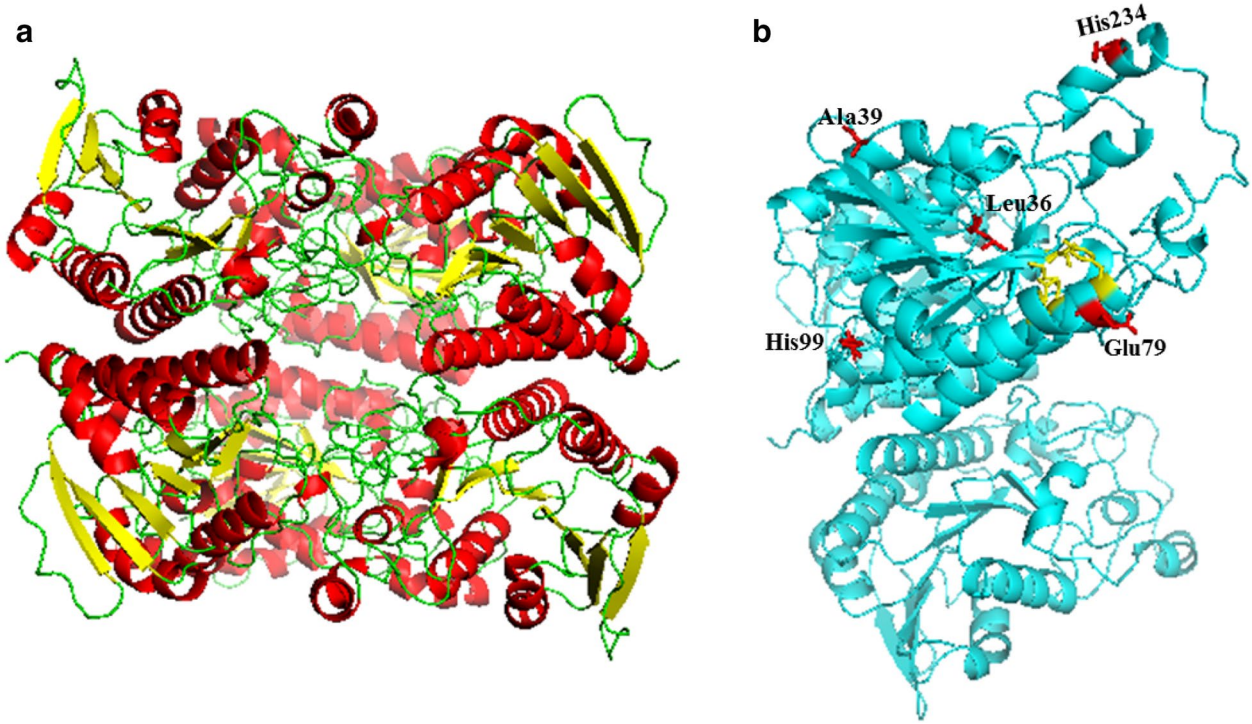

Fig. 2 Structural model of AtLBA4404 UDH. **a** Cartoon representation of the overall AtLBA4404 UDH structure. **b** The mutated amino acids are shown in red, the catalytic center in yellow (86Asn, 109Ser, 134Tyr, 138Lys)

Stability assay

In this study, the T_{50}^{10} value of the purified wild-type enzyme was 58 °C, but the kinetic stability improved markedly for three double or triple variants (A39P/H99Y, A39P/H234K and A39P/H99Y/H234K), while improving slightly for the single mutants A39P, H99Y and H234K. Especially promising was the T_{50}^{10} value for A39P/H99Y/H234K, which increased to 63 °C, a difference of 5 °C compared to wild-type (Table 2). We also determined the activity of the variant A39P/H99Y/H234K compared to wild-type UDH after incubation for various times at 58 °C. The first-order kinetics of both enzymes was obtained by measuring residual activity at 59 °C. As shown in Fig. 5, the activity of A39P/H99Y/H234K increased by more than 50% in the first minute compared to wild-type UDH, then dropped in the next two minutes. Over the next 60 min, the activity fell to 53% of the initial activity, and then maintained 50% activity for another 60 min at 59 °C. Even after 400 min at 59 °C, the A39P/H99Y/H234K variant retained more than 25% of the initial activity. Hence, the $t_{1/2}$ of A39P/H99Y/H234K improved approximately 400-fold compared to wild-type UDH, from 18 s to 120 min at 59 °C. The specific activity of the variants also improved, with A39P/H99Y/H234K

Table 1 Kinetic parameters of UDH from wt and mutants toward substrate glucuronic acid

Mutants	k_{cat} ($10^2 s^{-1}$)	K_m (mM)	k_{cat}/K_m (10^2 s^{-1} mM^{-1})	Specific activity (U mg^{-1})	Relative activity (100%)
WT	1.61 ± 0.3	0.20 ± 0.06	8.0	85 ± 2.1	100.0 ± 3.2
A39P	1.92 ± 0.5	0.26 ± 0.03	7.3	88 ± 3.1	103.5 ± 2.6
H99Y	1.79 ± 0.4	0.23 ± 0.05	7.7	93 ± 4.1	109.6 ± 3.4
H234K	1.95 ± 0.2	0.24 ± 0.03	8.1	110 ± 3.1	129.4 ± 2.9
A39P/H99Y	2.39 ± 0.1	0.20 ± 0.04	7.2	124 ± 2.9	146.8 ± 3.2
A39P/H234K	2.95 ± 0.4	0.18 ± 0.06	8.4	140 ± 3.6	165.7 ± 3.5
H99Y/H234K	3.18 ± 0.5	0.17 ± 0.05	8.6	149 ± 1.9	175.4 ± 2.9
A39P/H99Y/H234K	3.8 ± 0.7	0.15 ± 0.03	9.1	210 ± 3.0	247.6 ± 3.5

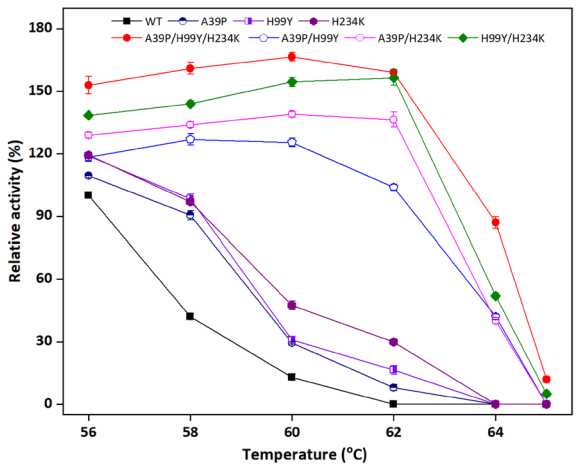

Fig. 3 Stability of wild-type UDH and all three variants, measured by the decrease in initial activity after 10 min incubation at the temperatures indicated. 100% activity is the activity of each enzyme incubated at optimum temperature for 30 min. A39P/H99Y/H234K, A39P/H234K and H99Y/H234K showed heat activation profiles

showing a 2.5-fold at 30 °C (210 U/mg) compared to wild-type (Table 1).

Bioconversion of GlcA with purified UDH

The bioconversion of the substrate GlcA by UDH was carried out for over 200 min at 37 °C to determine the yield of GA obtained, which was assessed by NMR (Additional file 1: Fig. S5), using the enzyme variants. The titer of GA was significantly higher for both the H99Y/H234K and A39PH99Y/H234K variants in the first 90 min ($p < 0.01$), then slowly continued to improve and still had not reached a maximum after 200 min. The final titer of GA was 27 mM ± 0.05 at 200 min for A39P/H99Y/H234, and 24 mM ± 0.10 at 200 min for H99Y/H234. Wild-type, H99Y/H234K and A39P/H99Y/H234K UDH demonstrated GA yields of 70%, 80% and 90%, respectively (Fig. 6).

Discussion

Compared with previous research, the UDH mutant produced in this study by rational evolution has both higher thermostability and improved activity (Table 3). After generating various single and combined mutations, we found that the best mutant (A39P/H99Y/H234K) had a 400-fold improvement in half-life at 58 °C, higher kinetic stability ($\Delta T_{50}^{30} = 5$ °C) and 2.5-fold higher specific activity at 30 °C than wild-type UDH.

The sites chosen for mutagenesis were located near the catalytic center (< 10 Å distant) and had good exposure to solvent (default value ≥ 30) (Eijsink et al. 2004; Kokkinidis et al. 2012; Wintrode et al. 2003). These positions (L36, A39, E79, H99, H234) were identified. In comparison with wild-type, H234K showed higher thermostability; while, A39P and H99Y were only slightly more thermostable. The triple mutant showed a greater improvement in thermostability than the sum of its three constituent

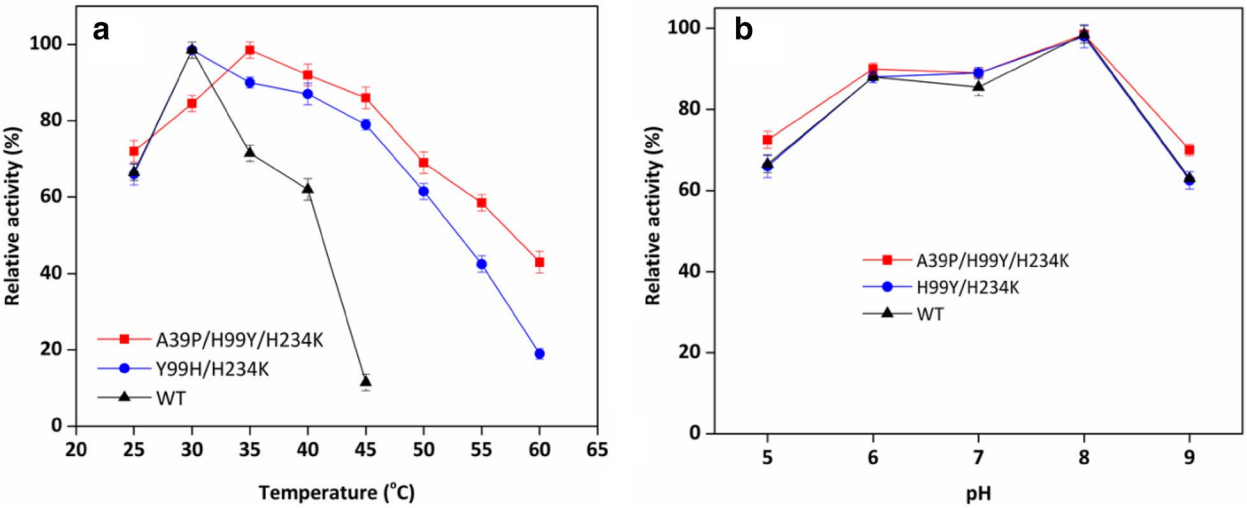

Fig. 4 Optimal temperature and pH values of UDH mutants. (**a**) Optimal temperature was determined in pH 8.0 buffer. (**b**) Optimal pH was determined at 37 °C except for H99Y/H234K and wild-type UDH (30 °C)

Table 2 Thermostability and activity parameters of wild-type and mutants of AtLBA 4404 UDH

Enzyme	Relative activity (30 °C)	$t_{1/2}$ (min) (59 °C)	Improvement of $t_{1/2}$ (59 °C)	ΔT_{50}^{10}
WT	85 ± 2.1	0.30 ± 0.02	1	0
A39P	88 ± 3.1	0.60 ± 0.1	1.8	0
H99Y	93 ± 4.1	1.30 ± 0.5	4.3	2
H234K	110 ± 3.1	5.10 ± 1.1	17	2.5
A39P/H99Y	124 ± 2.9	1.10 ± 0.5	3.5	3
A39P/H234K	140 ± 3.6	6.30 ± 1.9	21	3.5
H99Y/H234K	149 ± 1.9	16.00 ± 2.5	53	4
A39P/H99Y/H234K	210 ± 3.0	120 ± 3.5	400	5

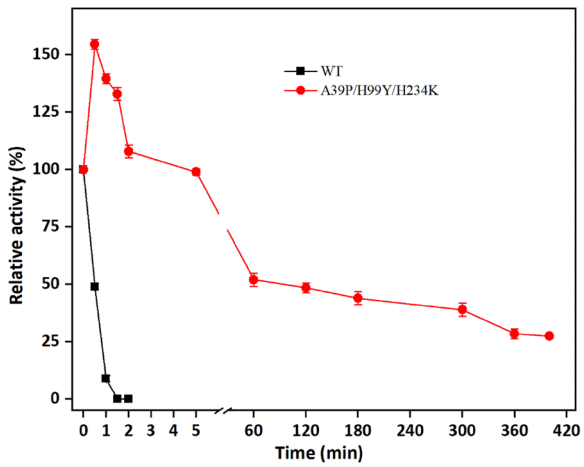

Fig. 5 Kinetic stability of the wild-type UDH and the triple mutant (A39P/H99Y/H234K) at 59 °C. Remaining activity was measured at 30 °C and 37 °C for the wild-type UDH and the triple mutant (A39P/H99Y/H234K)

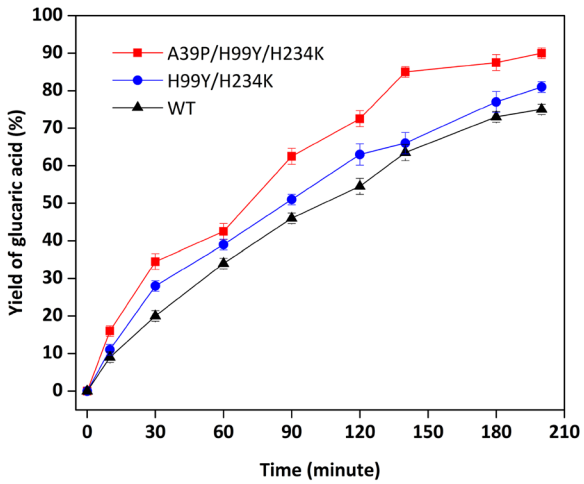

Fig. 6 Oxidative conversion of glucuronic acid to glucaric acid

individual mutations, demonstrating a positive synergistic effect. This reflects similar observations in the literature (Istomin et al. 2010; Reetz et al. 2010; Reetz 2013).

The three mutations (A39P, H99Y and H234K) combined within our best variant UDH (A39P/H99Y/H234K) are all located on the surface of the enzyme. It is well known that mutations that increase the thermostability are often found in surface regions (Eijsink et al. 2004; Wintrode et al. 2003; Stellwagen and Wilgus 1978). The mechanisms underlying the effect of these three mutations on thermostability can be rationalized by analysis of the enzyme structure (Deng et al. 2014; Samuel et al. 2018). Thus, the A39P mutation is stabilizing because proline can disrupt alpha-helix and beta-sheet, but is less of a problem at the surface; on the other hand, it is more prevalent in the proteins of thermophilic organisms, and lowers the conformational entropy (Wu et al. 2017; Ruller et al. 2010). Similarly, the tyrosine residue introduced in the H99Y mutant contains aromatic group, which can contribute to improve protein thermostability (Burley and Petsko 1985). For the H234K mutant, replacing histidine with lysine can enhance the formation of helices with a low cut-off, which could result in the improvement of thermostability (Wijma et al. 2013).

Additionally, increased thermostability, any engineered version of UDH would ideally also have higher catalytic activity to be of value to industry. However, directed evolution studies have suggested that these two characteristics, thermostability and activity, cannot both be optimized for an enzyme due to a stability–activity trade-off (Giver et al. 1998). Nevertheless, this trade-off has been challenged by protein engineering using genetic or chemical methods (Nguyen et al. 2017). Indeed, it has been suggested that a polyphosphate glucokinase (PPGK) mutant shows good compatibility between thermostability and activity after four rounds of directed evolution (Zhou et al. 2018). In our study, we found that both thermostability and activity showed a marked improvement in the A41P/H101Y/H236K UDH mutant derived from AtLBA4404. Similarly, a previously reported triple variant derived from AtC58, A41P/H101Y/H236K showed significantly improved thermostability; however, this mutant showed no enhancement in activity (Roth et al. 2017). The reasons for this difference might be as follows: (a) although the UDH from *A. tumefaciens* LBA4404 is very similar to that from *A. tumefaciens* C58, it is not identical. As shown in Additional file 1: Fig. S1, the differences between *A. tumefaciens* LBA4404 UDH and *A. tumefaciens* C58 UDH are mainly on C terminus,

Table 3 Comparison of enzymatic properties of characterization UDH

Strain	Specific activity (U/mg)	Half lifetime	References
A. tumefaciens C58	67 (pH 8.0, 30 °C)	50 min (pH 8.0, 37 °C)	Istomin et al. (2010)
P. putida KT2440	68 (pH 8.0, 30 °C)	30 min (pH 8.0, 37 °C)	Deng et al. (2014)
A. tumefaciens GV3101	73 (pH 8.0, 30 °C)	55 min (pH 8.0, 37 °C)	This study
A. tumefaciens EHA105	70 (pH 8.0, 30 °C)	55 min (pH 8.0, 37 °C)	This study
P. naphthalenivorans	80 (pH 8.0, 30 °C)	60 min (pH 8.0, 37 °C)	Kokkinidis et al. (2012)
T. bispora DSM43833	95 (pH 7.0, 50 °C)	60 min (pH7.0, 60 °C)	Komari et al. (2010)
A. tumefaciens LBA4404	86 (pH 8.0, 30 °C)	< 2 min (pH 8.0, 59 °C)	This study
A. tumefaciens LBA4404	210 (pH 8.0, 37 °C)	400 min (pH 8.0, 59 °C)	This study

which might be responsible for the different properties (Katoh et al. 2003; Li et al. 2018); (b) the *A. tumefaciens* LBA4404 used in our study is a model strain, and is often used in plant genetic transformation systems in the laboratory, which, to some extent, has led to the domestication of the strain, which might affect its genes and corresponding proteins (Aldemita and Hodges 1996; Komari et al. 2010). It is possible, therefore, that through the separate evolution and recombination of multiple independent characteristics, some rare mutations that improve both thermostability and activity at the same time could be identified under special conditions (Giver et al. 1998; Arnold et al. 2001).

Conclusions

In summary, we obtained a highly improved triple mutant (A39P/H99Y/H234K) of UDH, based on a homology model of AtLBA4404 UDH, by analysis of the catalytic center and subsequent surface engineering. The A39P/H99Y/H234K variant demonstrated a 400-fold better half-life time at 59 °C, higher kinetic stability ($\Delta T_{50}^{10} = 5$ °C) and 2.5-fold higher specific activity at 30 °C than wild-type UDH. The simultaneously improved specific activity and thermostability of this variant provides a novel alternative for the industrial production of GA from GlcA.

Supplementary information

Supplementary information accompanies this paper at https://doi.org/10.1186/s40643-019-0267-3.

Additional file 1. Additional tables and figures.

Abbreviations

UDH: uronate dehydrogenase; *E. coli*: *Escherichia coli*; At: *Agrobacterium tumefaciens*; *S. cerevisiae*: *Saccharomyces cerevisiae*; Inol: myo-inositol-1-phosphate synthease; MIOX: myo-inositol oxygenase; LB: Lysogeny Broth; PCR: polymerase chain reaction; WT: wild type; IPTG: isopropyl β-D-1-thiogalactopyranoside; GA: glucaric acid; GlcA: glucuronic acid.

Acknowledgements

Not applicable.

Authors' contributions

HHS, FP, PX and XLW carried out the experiments. HHS wrote the draft manuscript. WYL, MHZ and JGY participated in the design of the study and revision of the manuscript. All authors read and approved the final manuscript.

Funding

This work was funded by the National Natural Science Foundation of China (21676104, 21878105), the National Key Research and Development Program of China (2018YFC1603400, 2018YFC1602100), and the Science and Technology Program of Guangzhou (201904010360) for partially funding this work.

Availability of data and materials

The data on which the conclusions are all presented in this paper.

Ethics approval and consent to participate

Not applicable.

Consent for publication

Not applicable.

Competing interests

The authors declare that they have no competing interests.

Author details

[1] Laboratory of Applied Biocatalysis, School of Food Science and Engineering, South China University of Technology, Guangzhou 510640, People's Republic of China. [2] South China Institute of Collaborative Innovation, Xincheng Road, Dongguan 523808, People's Republic of China.

Received: 25 June 2019 Accepted: 28 August 2019
Published online: 23 September 2019

References

Aldemita RR, Hodges TK (1996) *Agrobacterium tumefaciens* mediated transformation of japonica and indica rice varieties. Planta 199:612–617

Alponti JS, Fonseca-Maldonado R, Ward RJ (2016) Thermostabilization of *Bacillus subtilis* gh11 xylanase by surface charge engineering. Int J Biol Macromol 87:522–528

Arnold FH, Wintrode PL, Miyazaki K, Gershenson A (2001) How enzymes adapt: lessons from directed evolution. Trends Biochem Sci 26:100–106

Bespalov VG, Aleksandrov VA (2012) Anticarcinogenic effect of potassium salts of glucaric and glucuronic acid in induced models of cervical and esophageal tumors. Vopr Onkol 58:537–540

Biasini M, Bienert S, Waterhouse A, Arnold K, Studer G, Schmidt T, Kiefer F, Cassarino TG, Bertoni M, Bordoli L, Schwede T (2014) Swiss-model: modelling protein tertiary and quaternary structure using evolutionary information. Nucleic Acids Res 42:W252–W258

Blair JA, Rauh D, Kung, Yun CH, Fan QW, Rode H, Zhang C, Eck MJ, Weiss WA, Shokat KM (2007) Structure-guided development of affinity probes for tyrosine kinases using chemical genetics. Nat Chem Biol 3:229–238
Burley SK, Petsko GA (1985) Aromatic-aromatic interaction: a mechanism of protein structure stabilization. Science 229:23–28
Deng Z, Yang H, Shin HD, Li J, Liu L (2014) Structure-based rational design and introduction of arginines on the surface of an alkaline α-amylase fromalkalimonas amylolyticafor improved thermostability. Appl Microbiol Biotechnol 98:8937–8945
Dwivedi C, Heck WJ, Downie AA, Larroya S, Webb TE (1990) Effect of calcium glucarate on β-glucuronidase activity and glucarate content of certain vegetables and fruits. Biochem Med Metab Biol 43:83–92
Eijsink VGH, Bjork A, Gaseidnes S, Sirevag R, Synstad B, Burg BVD, Vriend G (2004) Rational engineering of enzyme stability. J Biotechnol 113:105–120
Etzl S, Lindner R, Nelson MD, Winkler A (2018) Structure-guided design and functional characterization of an artificial red light-regulated guanylate/adenylate cyclase for optogenetic applications. J Biol Chem 293:9078–9089
Giver L, Gershenson A, Feskgard P, Arnold FH (1998) Directed evolution of a thermostable esterase. Proc Natl Acad Sci USA 95:12809–12813
Hoffmann F, Sotriffer C, Evers A, Xiong GM, Maser (2007) Understanding oligomerization in 3alpha-hydroxysteroid dehydrogenase/carbonyl reductase from *Comamonas testosteroni*: an in silico approach and evidence for an active protein. J Biotechnol 129:131–139
Istomin A, Gromiha MO, Jacobs D, Livesay D (2010) New insight into long-range nonadditivity within protein double-mutant cycles. Proteins 70:915–924
Katoh R, Nagata S, Misono H (2003) Cloning and sequencing of the leucine dehydrogenase gene form *Bacillus sphaericus* IFO3525 and importance of the C-terminal region for the enzyme activity. J Mol Catal B Enzym 23:239–247
Kokkinidis M, Glykos NM, Fadouloglou VE (2012) Protein flexibility and enzymatic catalysis. Adv Protein Chem Struct Biol 87:181–218
Komari T, Hiei Y, Saito Y, Murai N, Kumashiro T (2010) Vectors carrying two separate T-DNAs for co-transformation of higher plants mediated by *Agrobacterium tumefaciens* and segregation of transformants free from selection markers. Plant J 10:165–174
Kruger N (1988) The bradford method for protein quantitation. Methods Mol Biol 32:9–15
Li YX, Xue YM, Cao ZG, Zhou T, Alnadari F (2018) Characterization of a uronate dehydrogenase from *Thermobispora bispora* for production of glucaric acid from hemicellulose substrate. World J Microbiol Biotechnol 34:102
Moon TS, Yoon SH, Lanza AM, Roy-mayhew JD, Prather KL (2009) Enhancing production of glucaric acid from a synthetic pathway in recombinant escherichia coli. Appl Environ Microbiol 75:589–595
Morton DW, Kiely DE (2000) Evaluation of the film and adhesive properties of some block copolymer polyhydroxypolyamides from esterified aldaric acids and diamines. J Appl Polym Sci 77:3085–3092
Nguyen V, Wilson C, Hoemberger M, Stiller JB, Agafonov RV, Kutter S, Theobald DL, Kern D (2017) Evolutionary drivers of thermoadaptation in enzyme catalysis. Science 355:289–294
Parkkinen T, Boer H, Janis J, Andberg M, Penttila M, Koivula A, Rouvinen J (2011) Crystal structure of uronate dehydrogenase from agrobacterium tumefaciens. J Biol Chem 286(31):27294–27300
Pick A, Schmid J, Sieber V (2015) Characterization of uronate dehydrogenases catalysing the initial step in an oxidative pathway. Microb Biotechnol 8:633–643
Reetz MT (2013) The importance of additive and non-additive mutational effects in protein engineering. Angew Chem Int Ed 52:2658–2666
Reetz MT, Soni P, Acevedo JP, Sanchis J (2010) Creation of an amino acid network of structurally coupled residues in the directed evolution of a thermostable enzyme. Angew Chem Int Ed 48:8268–8272
Roth T, Beer B, André P, Sieber V (2017) Thermostabilization of the uronate dehydrogenase from *Agrobacterium tumefaciens* by semi-rational design. AMB Express 7:103
Ruller R, Deliberto L, Ward R (2010) Thermostable variants of the recombinant xylanase A from *Bacillus subtilis* produced by directed evolution show reduced heat capacity changes. Proteins 70:1280–1293
Samuel S, Jörg C, Volker S (2018) Structure-guided engineering of α-keto acid decarboxylase for the production of higher alcohols at elevated temperature. Chemsuschem 11:3335–3344
Stellwagen E, Wilgus H (1978) Relationship of protein thermostability to accessible surface area. Nat 275:342–343
Sutiono S, Carsten J, Sieber V (2018) Structure-Guided Engineering of α-Keto Acid Decarboxylase for the production of higher alcohols at elevated temperature. ChemSusChem 11(18):3335–3344
Tanner JJ, Hecht RM, Krause KL (1996) Determinants of enzyme thermostability observed in the molecular structure of thermusaquaticusd-glyceraldehyde-3-phosphate dehydrogenase at 2.5 Å resolution. Biochem 35:2597–2609
Thomas JL, Mason JI, Brandt S, Spencer BR, Norris W (2002) Structure/function relationships responsible for the kinetic differences between human type 1 and type 2 3 beta-hydroxysteroid dehydrogenase and for the catalysis of the type 1 activity. J Biol Chem 277:42795–42801
Wagner G, Hollmann S (1976) Uronic acid dehydrogenase from *Pseudomonas syringae*. J Biochem 61:589–596
Wagschal K, Jordan DB, Lee CC, Younger A, Braker JD, Chan VJ (2015) Biochemical characterization of uronate dehydrogenases from three *Pseudomonads*, *Chromohalobacter salixigens*, and *Polaromonas naphthalenivorans*. Enzyme Microb Technol 69:62–68
Walaszek Z (1990) Potential use of D-glucaric acid derivatives in cancer prevention. Cancer Lett 54(1–2):1–8
Werpy TA, Holladay JE (2004) White JF (2004) Top value added chemicals from biomass: I. Results of screening for potential candidates from sugars and synthesis gas. Synthetic Fuels 1:263–275
Wijma HJ, Floor RJ, Janssen DB (2013) Structure- and sequence-analysis inspired engineering of proteins for enhanced thermostability. Curr Opin Struct Biol 23:588–594
Wintrode PL, Zhang D, Vaidehi N, Arnold FH, Iii WAG (2003) Protein dynamics in a family of laboratory evolved thermophilic enzymes. J Mol Biol 327:745–757
Wu ZY, Deng WF, Tong YP, Liao Q, Xin DM, Yu HS, Feng J, Tang LX (2017) Exploring the thermostable properties of halohydrin dehalogenase from *Agrobacterium radiobacter* AD1 by a combinatorial directed evolution strategy. Appl Microbiol Biotechnol 101:3201–3211
Yang DF, Wei YT, Huang RB (2007) Computer-aided design of the stability of pyruvate formate-lyase from *Escherichia coli* by site-directed mutagenesis. Biosci Biotechnol Biochem 71:746–753
Yoon SH, Moon TS, Iranpour P, Lanza AM, Prather KJ (2009) Cloning and characterization of uronate dehydrogenases from two *Pseudomonads* and *Agrobacterium tumefaciens* strain c58. J Biotechnol 191:1565–1573
Zajic JE (1959) Hexuronic dehydrogenase of *Agrobacterium tumefaciens*. J Bacteriol 78:734–735
Zhang XF, Yang GY, Zhang Y, Xie Y, Withers SG, Feng Y (2016) A general and efficient strategy for generating the stable enzymes. Sci Rep 6:33797
Zhou W, Huang R, Zhu Z, Zhang Y (2018) Coevolution of both thermostability and activity of polyphosphate glucokinase from *Thermobifida fusca* YX. Appl Environ Microbiol 84:e01224
Zhu QQ, He WH, Kong XD, Fan LQ, Zhao J, Li SX, Xu JH (2014) Heterologous overexpression of vigna radiata, epoxide hydrolase in escherichia coli, and its catalytic performance in enantioconvergent hydrolysis of *p*-nitrostyrene oxide into (r)-p-nitrophenyl glycol. Appl Microbiol Biotechnol 98:207–218
Zółtaszek R, Hanausek M, Kiliańska ZM, Walaszek Z (2008) The biological role of D-glucaric acid and its derivatives: potential use in medicine. Postepy Hig Dosw 62:451–642

Publisher's Note